Do the Ends Justify the Mean? Proline Mutations at the Ends of the Keratin Coiled-Coil Rod Segment Are More Disruptive than Internal Mutations

Anthony Letai, Pierre A. Coulombe, and Elaine Fuchs

Howard Hughes Medical Institute, Departments of Molecular Genetics and Cell Biology, and Biochemistry and Molecular Biology, The University of Chicago, Chicago, Illinois 60637

Abstract. Intermediate filament (IF) assembly is remarkable, in that it appears to be self-driven by the primary sequence of IF proteins, a family (40–220 kd) with diverse sequences, but similar secondary structures. Each IF polypeptide has a central 310 amino acid residue α-helical rod domain, involved in coiled-coil dimer formation. Two short ($\sim$10 amino acid residue) stretches at the ends of this rod are more highly conserved than the rest, although the molecular basis for this is unknown. In addition, the rod is segmented by three short nonhelical linkers of conserved location, but not sequence. To examine the degree to which different conserved helical and nonhelical rod sequences contribute to dimer, tetramer, and higher ordered interactions, we introduced proline mutations in residues throughout the rod of a type I keratin, and we removed existing proline residues from the linker regions. To further probe the role of the rod ends, we introduced more subtle mutations near the COOH-terminus. We examined the consequences of these mutations on (*a*) IF network formation in vivo, and (*b*) 10-nm filament assembly in vitro. Surprisingly, all proline mutations located deep in the coiled-coil rod segment showed rather modest effects on filament network formation and 10-nm filament assembly. In addition, removing the existing proline residues was without apparent effect in vivo, and in vitro, these mutants assembled into 10-nm filaments with a tendency to aggregate, but with otherwise normal appearance. The most striking effects on filament network formation and IF assembly were observed with mutations at the very ends of the rod. These data indicate that sequences throughout the rod are not equal with respect to their role in filament network formation and in 10-nm filament assembly. Specifically, while the internal rod segments seem able to tolerate considerable changes in α-helical conformation, the conserved ends seem to be essential for creating a very specific structure, in which even small perturbations can lead to loss of IF stability and disruption of normal cellular interactions. These findings have important implications for the disease Epidermolysis Bullosa Simplex, arising from point mutations in keratins K5 or K14.

TOGETHER with actin microfilaments and microtubules, intermediate filaments (IF)[1] form the cytoskeleton of eukaryotic cells, comprising up to 85% of the total cellular protein. The basic subunit structure of all IF proteins is a coiled-coil dimer composed of two chains, each with a central $\sim$310 amino acid rod domain, which is largely α-helical and contains heptad repeats of hydrophobic residues (for reviews see Aebi et al., 1988; Steinert and Roop, 1988). Most IFs assemble into homopolymers, but keratin IFs are composed of heterodimers of type I and type II proteins, which associate to form tetramers (Coulombe and Fuchs, 1990; Hatzfeld and Weber, 1990*a*; Steinert, 1990; see also Franke et al., 1983). A series of higher ordered interactions among tetramers gives rise to 10-nm filaments, each composed of $\sim$20,000 IF molecules.

Given the common structure among IFs, it is surprising that different types of IF proteins have considerable sequence heterogeneity (for review see Steinert and Roop, 1988). The head and tail sequences flanking the α-helical rod are highly divergent both in size and in sequence. The sequence of the central rod segment classifies the IF type, and among different types, sequence identities throughout this domain average only $\sim$25–30%. However, the carboxy and amino ends of the rod exhibit remarkable conservation, even across IF types. The sequence TYRR/KLLEGE at the carboxy end of the rod domain is nearly unchanged among IF proteins.

Recently, several laboratories have conducted deletion and site-mutagenesis studies to begin to elucidate how different IF domains might be involved in IF network formation in

1. *Abbreviations used in this paper*: EBS, epidermolysis bullosa simplex; IF, intermediate filament; IFAP, IF associated protein; P, proline.

vivo (Albers and Fuchs, 1987, 1989; Lu and Lane, 1990; Gill et al., 1990; Wong and Cleveland, 1990; Christian et al., 1990; Heald and McKeon, 1990) and in 10-nm filament assembly in vitro (Coulombe et al., 1990; Hatzfeld and Weber, 1990*a*,*b*, 1991). From these studies, it is apparent that the highly variable nonhelical end domains flanking the rod segment have specialized roles, and the extent to which they contribute to IF network formation and/or 10-nm filament assembly is dependent upon the specific IF protein examined. In contrast, carboxy and amino terminal deletion studies have demonstrated that the ends of the rod domain seem to be universally essential, a finding substantiated by in vivo analysis of a number of point mutations in the carboxy end of the rod domain of nuclear lamin A (Heald and McKeon, 1990) and in vitro reconstitution studies of two mutations in a similar region of keratins K8 and/or K18 (Hatzfeld and Weber, 1991).

While the mutagenesis experiments conducted thus far have emphasized the importance of the rod segment in IF assembly, complementary internal rod mutations are necessary to provide insights into why these end domains are so highly evolutionarily conserved, and what might be their relevance relative to the internal rod segments. In this regard, it is interesting that the rod is not uniformly α-helical. The α-helical rod is segmented by two short nonhelical linkers (termed LI and LII in this paper) of conserved location, but variable sequence. Among IFs, these linkers frequently contain proline and glycine residues, which are predicted to destabilize the α-helix and perturb potential coiled-coil interactions (Hanukoglu and Fuchs, 1982, 1983; Geisler and Weber, 1982; for review see Aebi et al., 1988; Steinert and Roop, 1988). Some IFs, predominantly keratins, have a third linker (LIII), which appears less disruptive, containing glycine but no proline residues (Hanukoglu and Fuchs, 1982, 1983). The role of the linkers in 10-nm filament assembly is unknown, as is a knowledge of whether other segments of the α-helical rod segment might be able to tolerate such strong helix-perturbing residues.

Thus far, only two mutations (Lys/Arg-->Val) located outside (25–35 residues internal to) the highly conserved end domains of the rod have been analyzed, and these had no effect on nuclear lamina formation in vivo (Heald and McKeon, 1990). While intriguing, one of these mutations (Lys-->Val) merely restored a natural difference between lamin and K14 (V380), and neither of these mutations were helix-perturbing residues. Thus, assessing the relative importance of even this small internal rod segment was not possible, given the small number of internal mutants tested, the relatively mild nature of the substitutions and the existence of similar null mutations in the conserved ends of the lamin rod (Heald and McKeon, 1990).

To begin to investigate the effects of helix-perturbing residues on the four helical segments of IF proteins, and the possible roles of the existing proline residues, we (*a*) engineered nine proline substitutions within conserved segments of the α-helical rod domain of the human keratin K14, and (*b*) removed the prolines within the rod. K14, along with its partner keratin K5, forms the 10-nm filament network of keratinocytes in a variety of stratified squamous epithelia (Nelson and Sun, 1983). K14 mutants were tested by transient gene transfection into cultured epidermal and simple epithelial cells and by in vitro filament assembly with wild-type K5. Using more extensive and subtle mutations, we then investigated critical segments of the rod in more depth. Collectively, our results demonstrate for the first time that (*a*) the highly conserved ends of the rod play a greater role in 10-nm filament assembly and IF network formation than the internal segments, and (*b*) the internal rod segment can accommodate considerably more deformation than was previously realized. These studies have important implications for the wide variability in severity of the genetic skin disease epidermolysis bullosa simplex (*EBS*), which arises from point mutations in the human genes encoding K5 and K14.

Materials and Methods

Cell Culture and Gene Transfections

Keratinocytes and PtK2 cells were cultured, transfected, fixed, and processed for immunofluorescent labeling as described previously (Albers and Fuchs, 1987). The antisera used were a rabbit polyclonal anti-P against the COOH-terminal neuropeptide substance P tag (Wako Chemicals, Richmond, VA), guinea pig polyclonal anti-K5 antibodies against the human K5 COOH-terminal peptide (Lersch, R., and E. Fuchs, unpublished data), and a mouse mAb, anti-K8, against the endogenous PtK2 network (Lane et al., 1982). To visualize primary antibodies, we used FITC-conjugated goat anti-rabbit IgG (Cappel Biochemicals, Durham, NC) and Texas red-conjugated goat anti-guinea pig or anti-mouse IgG (Accurate Biochemicals, Westbury, NY).

IF Extractions and Immunoblot Analysis

Keratins were isolated from transiently transfected cells and subjected to SDS-PAGE and immunoblot analysis as described previously (Albers and Fuchs, 1987).

Analysis of Intermediate Filament Proteins

Bacterially expressed keratins were isolated from inclusion bodies and purified by anion exchange chromatography as previously described (Coulombe and Fuchs, 1990). In vitro filament assembly assays were carried out as described (Coulombe and Fuchs, 1990), with the exception that filament reconstitution was initiated in assembly buffer containing 9 M rather than 6.5 M urea, and 0.5 mM $MgCl_2$ was added to the final dialysis solution (Eckert, B. S., and P. L. Yeagle. 1990. *J. Cell Biol.* 111:433*a*). Assembled filaments were negatively stained (1.25% uranyl acetate) and examined by EM. Assembly efficiency was routinely examined by centrifugation of protein mixtures before and after assembly at 20,000 *g* for 60 min, followed by analysis of pellet and supernatant by SDS-PAGE.

Mutagenesis

Point mutations were engineered in a bluescript-KS+ plasmid (Stratagene, La Jolla, CA) containing the wild-type K14 cDNA. Mutants were generated using either (*a*) the site-directed mutagenesis protocol described by Kunkel (1985), or (*b*) direct insert of paired mutagenized oligonucleotides. A fragment encompassing the mutation was then subcloned into either pJK14P (SV-40 promoter/enhancer-based mammalian expression vector; Albers and Fuchs, 1987) or pETK14P (bacterial expression vector; Coulombe and Fuchs, 1990).

Results

Selection of Proline Mutations and Preparation of Keratinocyte Expression Vectors

Fig. 1 illustrates the predicted secondary structure for human K14, depicting the four α-helical domains separated by the three nonhelical linker regions (see Hanukoglu and Fuchs, 1982 for secondary structure analyses). To determine whether the K14 polypeptide might be able to tolerate helix-

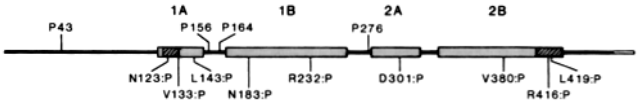

Figure 1. Stick diagram of existing and genetically engineered proline residues in the human K14 keratin, depicting their location relative to the α-helical rod domain. For K14, the rod domain is ~310 amino acid residues and is subdivided into four segments (helix 1A, helix 1B, helix 2A, and helix 2B) based upon the presence of proline or multiple glycine residues in the short nonhelical stretches linking these segments (Hanukoglu and Fuchs, 1982; Coulombe et al., 1990). The helices are denoted by boxes, with the hatched regions denoting the most highly evolutionarily conserved segments. The black bars denote the nonhelical domains; thin white bar denotes the neuropeptide substance P tag. The naturally occurring proline (*P*) residues are indicated along the top; the genetically engineered proline mutations are shown along the bottom. Point mutants were engineered in the K14 cDNA by site-directed mutagenesis using either the Kunkel method (1985), or synthetic oligonucleotide inserts. In all cases, mutations were verified by DNA sequencing.

perturbing residues within the four helices, we used site-directed mutagenesis (Kunkel, 1985) to engineer proline substitutions in each of the four segments. A comparison of published IF sequences from invertebrates to mammals revealed that the most highly conserved residue at the amino end of the rod is K14 N123, present in 64 of 64 IF sequences. We engineered a proline mutation, N123:P, in this highly conserved site. At the carboxy terminus, TYRR/KLLEGE is present in nearly all IF proteins (residues 414-422, respectively, in human K14; Marchuk et al., 1984). Since L419 is the first residue in the last heptad repeat of the rod domain, we engineered L419:P. Finally, since the equivalent of R416 is an R in 73 of 75 IFs, we made R416:P.

Fig. 1 illustrates the relative positions of the nine encoded proline (P) residues that were introduced individually into the rod segments. To drive expression of these mutant K14 cDNAs in a variety of cultured cell types, we used the major early promoter and enhancer of the SV-40 genome. To track the expression of the mutants in transfected keratinocytes in culture, we replaced the sequences encoding the five terminal antigenic residues of the wild-type K14 with sequences encoding the antigenic portion of the neuropeptide substance P (see Albers and Fuchs, 1987 for details). This enabled us to use an anti-P antibody to detect the transgene product and an anti-K14 or anti-K5 antibody to detect expression of the endogenous keratin filament network. The mutant proteins will be referred to as XN:Y, where X represents the K14 amino acid residue mutated, N represents the residue number based upon Marchuk et al., 1984, and Y represents the new amino acid residue created as a consequence of the mutation.

Proline Mutants at the Ends of the Rod Domain Have More Severe Effects than Internal Proline Mutants

To examine the behavior of our nine proline point mutants on keratin network formation in cultured keratinocytes (SCC-13; epidermal squamous cell carcinoma; $K5^+$, $K14^+$; Wu and Rheinwald, 1981), we transfected cells using the calcium phosphate precipitation method (Graham and Van der Eb, 1973). At 65 h after transfection, part of the cells were harvested for IF protein analysis, and the rest were fixed and stained for double immunofluorescence using anti-P and anti-K5.

As judged by the calculated percentage of brightly anti-P staining cells in populations transfected with each of our mutants, the transfection efficiency was typically 5%. When expressed in culture, nearly all of our mutant cDNAs produced stable and roughly comparable levels of the expected 52-kd protein (Fig. 2). The exception was D301:P (Fig. 2 *B*, lane 7). Since D301:P produced stable protein in bacteria (see below), but not in cultured epithelial cells, we suspected that this mutant might be prone to some proteolytic event. Consequently, we did not use this mutant for further culture studies.

The relative levels of all other point mutant K14 proteins were similar to that of K14P, as judged by SDS-PAGE and anti-P immunoblot analysis of IF proteins extracted from transfected cultures (Fig. 2, *A* and *B*, respectively). The amount of K14P relative to endogenous K14 protein was estimated using dilutions of known concentrations of bacterially expressed and purified K14P and K5 as standards. Taking into account that only 5% of the cells were judged to be transfected, it was estimated that the average level of mutant K14P in most transfected cells was ~20–35% of the endogenous level of K14 protein. Some variation in intensity of immunofluorescence staining was observed, indicating that absolute amounts of K14P in a given cell might deviate several-fold from the average value.

In transfected keratinocytes, mutant keratins containing proline mutations at the ends of the rod domain integrated into and perturbed the endogenous keratin filament network (Fig. 3 *A*, L419:P, anti-P; *B*, same cells, anti-K5). While filamentous cables were still seen, the network was often withdrawn from the cell periphery, and punctate staining was evident in the cytoplasm. This phenotype was seen for keratinocytes transfected with N123:P, V133:P, R416:P, and L419:P, and was present in >20% of transfected SCC-13 cells. The phenotype was distinctly different from that of wild-type K14P, which integrated into the keratin filament network without apparent perturbation in 100% of the cells (*C*, anti-P and *D*, anti-K5). Collectively, these findings suggested that proline mutations within the highly conserved end domains of the α-helical rod segment of K14 can cause major perturbations in keratin network formation. The studies were consistent with and extended those reported by Heald and McKeon (1990), who noted that certain point mutations, including the equivalent mutation of R416:P, in the carboxy end of the rod domain of nuclear lamin A altered the ability of lamins to form a proper nuclear envelope. The data were also consistent with deletion mutagenesis studies, showing that removal of these highly conserved end domains resulted in mutant IF proteins that perturbed filament network formation and 10-nm filament assembly (Albers and Fuchs, 1987, 1989; Coulombe et al., 1990; Gill et al., 1990; Lu and Lane, 1990; Wong and Cleveland, 1990). Finally, these findings were in agreement with Hatzfeld and Weber (1991), who examined the effects of two K8 and/or K18 point mutations at the COOH-terminal end of the rod domain on 10-nm filament assembly in vitro.

Unexpectedly, the internal proline mutations showed no visible perturbations on keratin filament networks in cultured keratinocytes. Thus, L143:P, N183:P, R232:P, and V380:P all integrated into the endogenous keratin filament

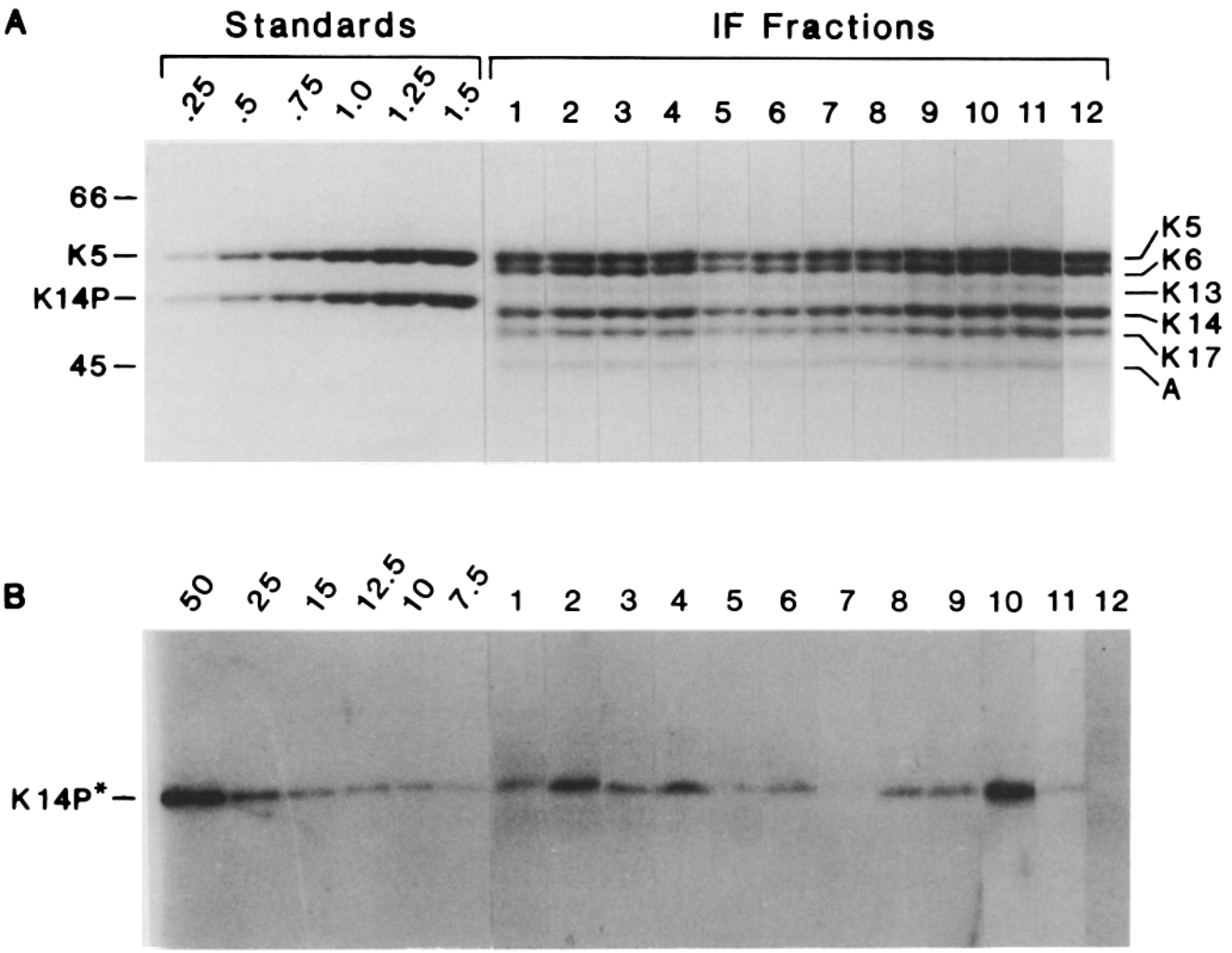

Figure 2. Accumulation of mutant keratins in transfected keratinocytes. SCC-13 keratinocytes (100-mm dishes) were transfected with K14P and 13 different K14P point mutants. At 65 h posttransfection, cells were harvested, and IF proteins were extracted (see Albers and Fuchs, 1987 for methods). Proteins were resolved by electrophoresis through 8.5% SDS-polyacrylamide gels. Gels were subjected to Coomassie blue staining (*A*) or immunoblot analysis with a rabbit polyclonal anti-P antiserum (1:700 dilution) (*B*). Bacterially expressed K5 and K14P were used as mass and immunoblot standards. (*A*). At left, K5 and K14P standards are shown at 0.25, 0.50, 0.75, 1, 1.25, and 1.5 μg, respectively. Lanes *1–12* contain 5 μg aliquots of IF proteins extracted from cells transfected with: lane *1*, K14P; lane *2*, N123:P; lane *3*, V133:P; lane *4*, L143:P; lane *5*, N183:P; lane *6*, R232:P; lane *7*, D301:P; lane *8*, V380:P; lane *9*, R416:P, lane *10*, L419:P; lane *11*, L419:R; lane *12*, Bluescript KS$^+$ plasmid (negative control). Migration of molecular mass standards of 45 and 66 kd are indicated at left. Keratin components of the IF preparations (*K5*, *K6*, *K13*, *K14*, and *K17*) as well as actin (*A*) are indicated at right. (*B*) At left, K5 and K14P standards were loaded at 50, 25, 15, 12.5, 10.0, and 7.5 ng, respectively. Lanes *1–12* contain 20-μg aliquots of IF proteins from cells transfected with: lane *1*, K14P; lane *2*, N123:P; lane *3*, V133:P; lane *4*, L143:P; lane *5*, N183:P; lane *6*, R232:P; lane *7*, D301:P; lane *8*, V380:P; lane *9*, R416:P; lane *10*, L419:P; lane *11*, L419:R; lane *12*, Bluescript KS$^+$. (*) Denotes location of the bands corresponding to K14P and K14P mutants, all of which migrated similarly on one dimensional SDS gels. Amounts (in ng) of total endogenous K14 and exogenous K14P proteins were estimated by comparison with mass standards on SDS-PAGE and immunoblots, respectively. The amounts of exogenous K14P proteins per transfected cell were estimated by dividing the total ng exogenous K14P protein by the percent of transfected cells in the population, a figure obtained by immunofluorescence labeling of cells grown on chamber slides and transfected in parallel with the cells used for IF assays. An average ratio of exogenous K14P protein to endogenous K14 protein per transfected cell could then be determined directly. Note: all mutants except for D301:P produced stable protein at comparable levels. It was estimated that on average, most of the transgenes were expressed at ~20–35% of the endogenous K14 levels under the conditions used.

network without apparent perturbations (Fig. 3, N183:P, *E*, anti-P and *F*, anti-K5). Despite the knowledge that the central portion of the rod domain is less highly conserved than the end segments, it has been generally predicted that proline mutations within the α-helical rod domain would have a deleterious effect on the α-helicity of the rod and subsequently on intermediate filament structure and filament network formation. While these findings did not rule out the possibility that certain internal proline mutations might lead to perturbations of the keratin filament network, they suggested that the rod segment was not uniform in its role in keratin network formation.

Epidermal keratin filament networks are notoriously stable and dense, comprising up to 30% of the total cell protein in cultured human keratinocytes (Sun and Green, 1978). To ascertain whether our internal proline mutations might have

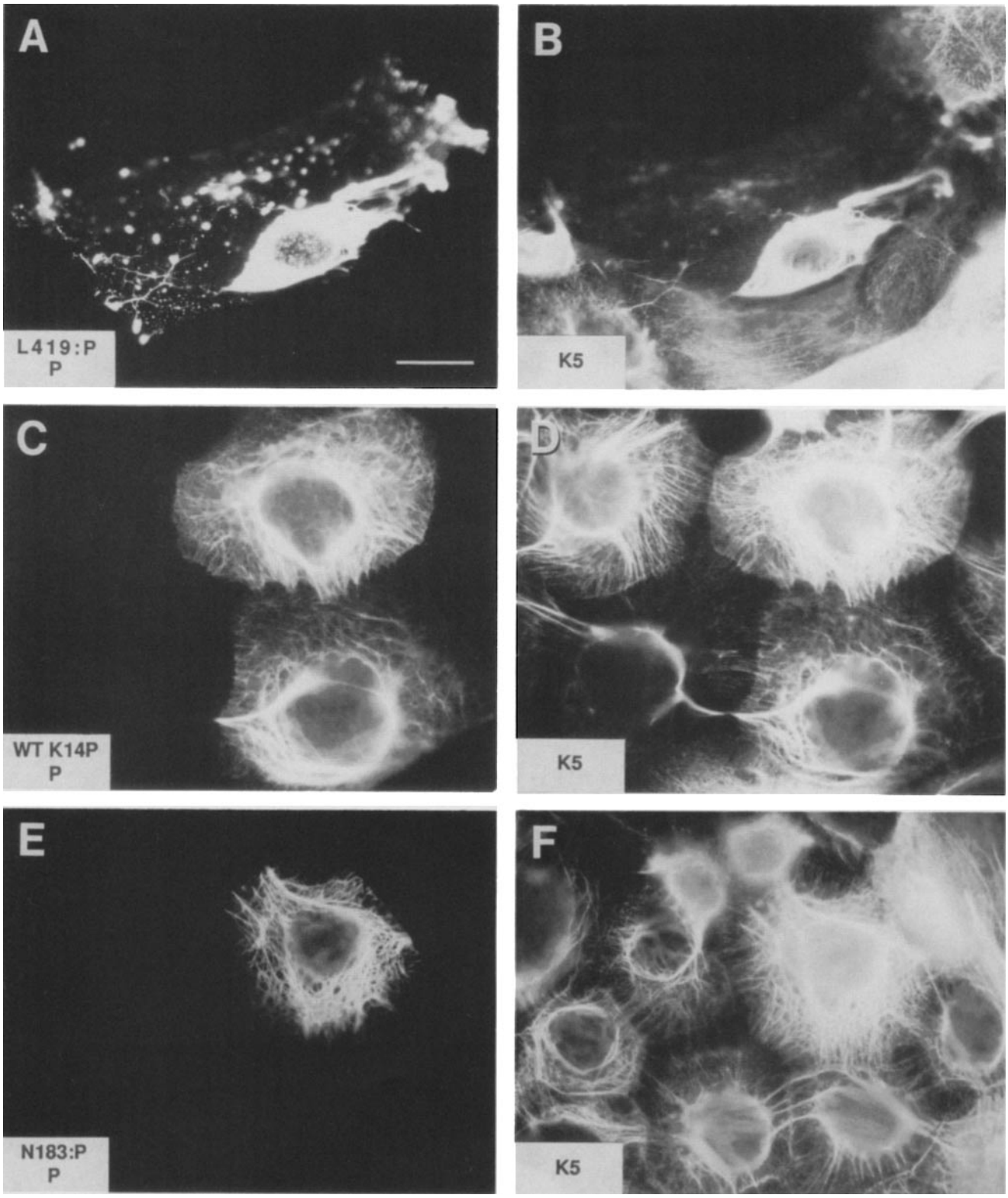

Figure 3. Immunofluorescence analysis of transfected keratinocytes expressing K14P proline mutants. SCC-13 keratinocytes were transfected with nine keratin point mutants. 65 h posttransfection, cells were fixed and co-stained with anti-P (first frame of each set) and anti-K5 (second frame of each set) antisera. SCC-13 cells shown were transfected with: (*A* and *B*) L419:P (note that in some cells, the keratin network has separated from the plasma membrane and is beginning to collapse toward the nucleus); this phenotype was also seen for N123:P, V133:P, and R416:P in >20% of the transfected cells; (*C* and *D*) K14P (wild-type); *E* and *F*, N183:P (this phenotype was indistinguishable from wild-type, and was also seen for L143:P, R232:P, D301:P, and V380:P). Bar, 20 μm.

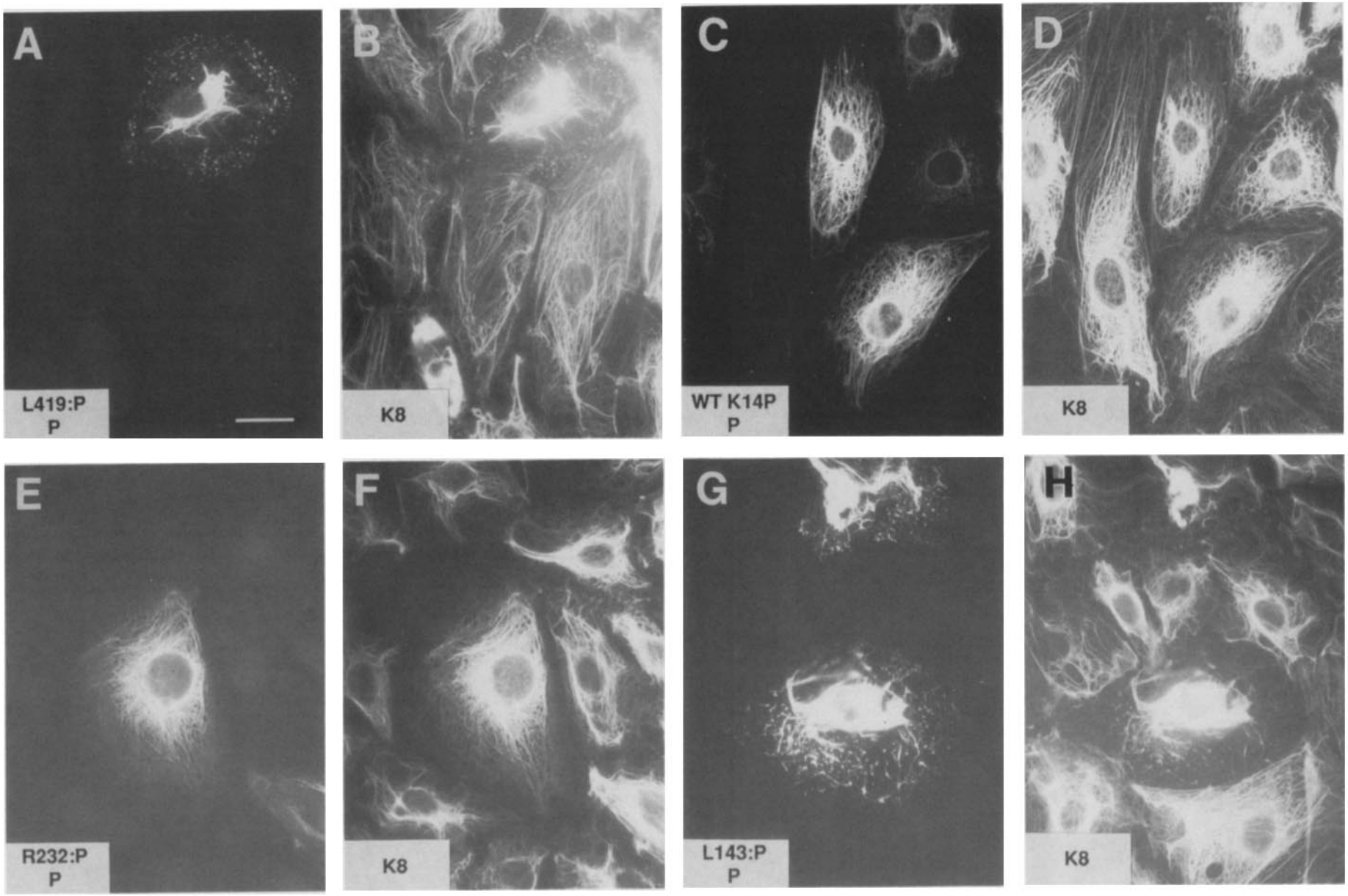
A
L419:P
P
B
K8
C
WT K14P
P
D
K8
E
R232:P
P
F
K8
G
L143:P
P
H
K8

subtle effects on keratin network formation that we could not detect in transfected keratinocytes, we repeated our transfections in rat potoroo (PtK2) kidney epithelial cells ($K8^+$, $K18^+$), which have significantly less abundant keratin networks (~5% of the total cell protein as judged by densitometry staining of Coomassie blue–stained gels), yielding a higher ratio of mutant/wild-type K14 in PtK2 than in SCC-13 cells. In addition, a reduced stability of the resulting IFs might be expected since K14 was forced to co-assemble with a foreign (K8) type II keratin (Franke et al., 1983; see also Albers and Fuchs, 1987).

As expected, all proline mutations near the ends of the rod exhibited gross perturbations in the filament networks, including withdrawal of the network from the cell periphery and/or complete perinuclear collapse in >50% of transfected PtK2 cells (Fig. 4, L419:P, *A*, anti-P and *B*, anti-K8; compare with wild-type K14P transfected PtK2 cells in *C* and *D*, respectively). Many of the mutant transfected cells exhibiting a wild-type network stained only weakly with anti-P antibodies, suggesting that these cells expressed lower levels of mutant protein than those with collapsed networks.

Despite the lesser stability of the PtK2 keratin network, four of the five internal K14 proline mutations still showed no apparent effect on the endogenous IF network of transfected cells (Fig. 4, R232:P, *E*, anti-P and *F*, anti-K8). Interestingly, however, the internal proline mutant L143:P perturbed the PtK2 network (Fig. 4, L143:P, *G*, anti-P and *H*, anti-K8). Since this mutant had shown no effect on the more stable SCC-13 keratin networks, it seems likely that it was intermediate in its ability to perturb keratin network formation in vivo.

No changes were detected in the other cytoskeletal networks of transfected cells (not shown, but see Albers and Fuchs, 1987, 1989 for similar analyses). Since these other networks are generally more sensitive to metabolic and cell cycle changes than are keratin networks, it is unlikely that the disruption involving keratin IFs at the cell periphery was caused by any non-specific global shock to the cell's normal functions.

Effects of Proline Mutants on Tetramer Formation and 10-nm Filament Assembly

To examine the effects of our point mutants on keratin filament assembly, we cloned the mutant cDNAs into a bacterial expression vector, enabling us to isolate and purify milligram quantities of mutant and wild-type K14P as well as the type II partner keratin, K5 (Coulombe and Fuchs, 1990; Coulombe et al., 1990). All of our mutants, including D301:P, produced stable protein of the predicted size (data not shown). As expected from previous analyses of truncated keratin mutants (Coulombe et al., 1990), all of these mutants assembled into heterodimers in 9 M urea buffer and heterotetramers in 6.5 M urea buffer, as judged by anion exchange chromatography followed by gel filtration chromatography (Coulombe and Fuchs, 1990). No difference in efficiency of tetramer formation was observed between any of the point mutants and wild-type K14 (data not shown; see Coulombe et al., 1990 for similar results with truncated K14 proteins). When dialyzed, heterotetramers of wild-type K5 and K14 proline mutants assembled into 10-nm filaments in vitro (Fig. 5). However, relative to wild-type K14P-K5 filaments (*A*), substantial perturbations were observed in all filament assembly reactions involving K14 mutants with proline substitutions near the rod ends (B–E). Interestingly, at least one of these mutants, L419:P had a more deleterious effect on keratin filament assembly than was seen previously for the deletion of the entire 418-LLEGE-422 sequence (see Coulombe et al., 1990 for deletion analyses).

Filaments composed of the rod-end mutants exhibited one or more of several different atypical characteristics, including short filament length, irregular width, roughness of filament surface, filament aggregation, and filament branching. Thus, at 250 μg/ml, wild-type keratins assembled into filaments which were routinely >2-μm long (*A*), while filaments formed from K5 and either L143:P, R416:P, or L419:P were significantly shorter, as evidenced by a >5× increase in the number of free filament ends seen in electron micrographs (see examples in *B*, L143:P). This feature was less pronounced for N123:P and V133:P. In addition, filaments composed of L143:P, R416:P, and L419:P, but not N123:P and V133:P, were somewhat irregular in width and showed some roughness, with small protuberances along the filament surface. Filaments made from all five rod-end mutants exhibited a propensity to aggregate, but this was particularly prominent for L419:P (*C*) and R416:P (not shown). Aggregation also seemed to be associated with an increased propensity of filaments to branch, a feature especially prominent in all of our rod end mutants (*D* shows examples for N123:P, *arrowheads* denote some of the numerous branchpoints). Although wild-type filaments showed occasional branching under the conditions used, these filaments consistently had a 5× greater tendency to do so. V133:P was unusual in its ability to generate filaments that associated laterally to form cable-like structures which frequently extended for hundreds of nanometers before separating again into component 10-nm filaments (*E*, regions denoted by *double arrowheads*). In addition, filaments composed of V133:P were rarely straight, but rather changed directions frequently, creating wavy patterns (see examples in *E*, compare with wild-type in *A*). For all of the aberrancies observed, the P-tag did not seem to be responsible, since removal of the tag from one mutant (L419:P) did not restore the phenotype.

Figure 4. Immunofluorescence analysis of transfected simple epithelial cells expressing K14 proline mutants. PtK2 cells were transfected with nine keratin point mutants. At 65 h posttransfection, cells were fixed and co-stained with anti-P (first of each set) and anti-K8 (second of each set). *A* and *B*, two L419:P-expressing PtK2 cells with keratin networks collapsed around the nucleus. This phenotype was also seen for mutants N123:P, V133:P and R416:P, in most transfected cells. Note: the collapsed keratin network phenotype was also characteristic of cells expressing D301:P, although we were unable to interpret this result due to the failure to obtain appreciable levels of this protein in transiently transfected cells. Consequently, it is possible that protein processing contributed to this phenotype. (*C* and *D*) PtK2 cell expressing K14P. (*E* and *F*) R232:P. This phenotype was also seen for N183:P and V380:P. (*G* and *H*) L143:P. Bar, 20 μm.

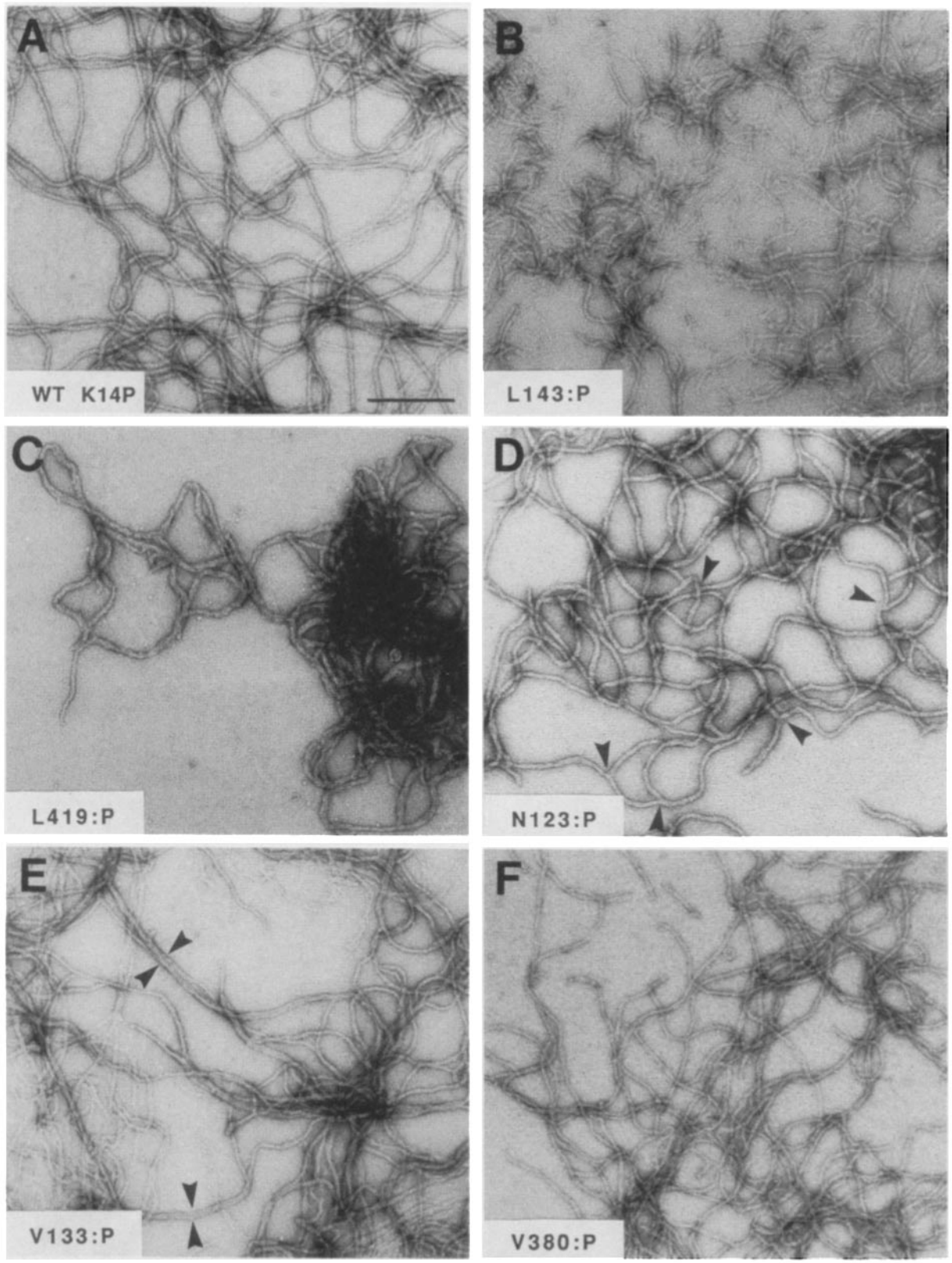

Figure 5. In vitro assembly of bacterially expressed K14 proline mutants into 10-nm filaments. 1:1 molar complexes of K5 and either K14P or K14P mutants were isolated by anion exchange chromatography, adjusted to 250 μg/ml in 9 M urea buffer, and subjected to in vitro filament assembly as outlined previously (Coulombe and Fuchs, 1990). Assembled filaments were applied to glow-discharged carbon-coated nickel grids, negatively stained with 1.25% uranyl acetate and visualized with a Phillips CM-10 electron microscope. Magnification was calibrated using a diffraction grating replica. Efficiency of assembly was estimated as described in the text. Filaments shown were assembled from K5 and: *A*, K14P (note wild-type appearance); *B*, L143:P (note shortness of filaments); *C*, L419:P (note shortness of filaments, irregular width and aggregation of filaments); *D*, N123:P (note numerous branchpoints, denoted by arrowheads, see also *C*); *E*, V133:P (note unusual waviness of filaments and propensity of intertwining of filaments into larger cable-like structures, denoted by opposing arrowheads); *F*, V380:P (note that these filaments are similar, but slightly shorter than the wild-type filaments shown in *A*). Bar, 200 nm.

Filaments formed from the five proline rod-end mutants were abundant, and only for L143:P, R416:P, and L419:P did the number of filaments seem appreciably reduced over wild-type reconstitution assays. Filament-forming efficiency was verified by taking keratin mixtures before and after assembly, and subjecting them to centrifugation at 20,000 *g* for 60 min, followed by analysis of the supernatant and pellet by SDS-PAGE. These conditions were known to leave keratin tetramers in the soluble pool (Coulombe and Fuchs, 1990). When compared with wild-type assembly mixtures, which left 5–10% keratins in the supernatant, only the L143:P assembly mixture left a significantly greater amount (>50%) of protein in solution (data not shown). A likely explanation as to why L419:P and R416:P did not leave large amounts of protein in solution is that these mutants produced filaments which aggregated substantially under the conditions used. Filament forming efficiency was further studied by reducing assembly mixtures to near critical concentrations (50 μg/ml) necessary for filament assembly. Under these more stringent conditions, all K14 proline mutants and wild-type K14 still assembled with wild-type K5 into 10-nm filaments. However, in all cases including wild-type K14, the filaments were significantly shorter at 50-μg/ml than at 250-μg/ml concentrations. Elongation was most strongly affected for the mutants L143:P and L419:P, which made filaments with an average length of only 100 nm, and with no filaments appreciably longer than this. In contrast, wild-type K14 and other end proline mutations produced filaments of ~200–400 nm, with a few filaments extending to lengths of >2 μm (data not shown). Collectively, these results indicated that the major perturbation common to all five of these mutants was on filament length and interfilament interactions, while some mutants showed in addition, effects on filament structure and filament forming efficiency.

In contrast to the proline mutations nearest the ends of the rod, the four more internal proline mutations, N183:P, R232:P, D301:P, and V380:P had significantly milder effects on filament assembly. These internal proline K14 mutants combined with wild-type K5 to efficiently produce 10-nm filaments that were nearly indistinguishable from wild type (Fig. 5 *F*, V380:P). It was only upon careful and extensive examination that we assessed that these filaments were somewhat shorter than normal. In addition, these filaments had a slightly greater tendency to aggregate and/or branch than normal (see *F*). In general, however, our in vitro assembly studies indicated that the internal proline mutants had a much milder effect on 10-nm filament assembly than the end domain proline mutants. Moreover, our in vitro studies were consistent with our in vivo transfection studies, demonstrating a correlation between the disruption of the keratin filament network in transfected cells, and the perturbations in assembled keratin filaments in vitro.

K14P Lacking Naturally Occurring Prolines and Glycines in Its Linker Segments Incorporates Into a Keratin Network and Forms Filaments with Seemingly Normal 10-nm Structure

Since structural perturbations caused by internal proline mutations did not seem to have marked effects on keratin network formation or 10-nm filament assembly, we wondered whether removing the naturally occurring proline residues might perturb keratin filament structure. To test this possibility, we sequentially substituted all of the natural internal proline residues (see diagram in Fig. 6). Without altering linker length, proline and glycine residues from linkers I and II (LI and LII) were replaced with residues compatible with the α-helical and coiled-coil motifs of the rest of the rod domain. Neither P156:R/P164:E (referred to as the LIα mutant) nor G262:N/G265:D/G266:V/P276:L/G277:R (referred to as the LIIα mutant) caused perturbations in the keratin filament networks when expressed in either SCC-13 or PtK2 cells. Even when the double mutant LIα/LIIα was expressed, it still integrated into SCC-13 and PtK2 networks in a fashion indistinguishable from wild-type K14 (Fig. 6, *A* and *B*, respectively). Thus, despite the evolutionary conservation of nonhelical linker position within the IF rod, removal of these internal proline residues did not seem to compromise the keratin filament network, at least in the context of an epithelial cell cultured on a plastic substratum.

To test for possible aberrations in keratin filament structure, the three linker mutants were then tested in our filament assembly assay. All three linker mutants assembled into 10-nm filaments exhibiting wild-type regularity in width, length and surface smoothness (Fig. 6, *C–E*). These filaments appeared no straighter or stiffer than those assembled from wild-type K14. However, filaments formed from each of the three linker mutants showed some propensity to aggregate. This tendency was slight with the LIα and LIIα mutants (*C* and *D*, respectively), but was quite striking with the double mutant, LIα/LIIα (*E*). However, when the starting concentration of keratin was reduced from 250 to 50 μg/ml, the aggregation was significantly reduced (data not shown).

A More Detailed Analysis of the End Domains

Having already demonstrated that end domain proline mutants had a potent effect on 10-nm filament assembly and keratin network formation, we wondered whether more subtle mutations might also perturb the α-helical rod in a fashion deleterious to assembly. We focused on the carboxy terminal end of the rod domain, where the sequence TYRR/KLLEGE is present in nearly all IF proteins. The mutations that we introduced are illustrated in Fig. 7. Since L419:P and R416:P were among the most deleterious of the nine proline mutants tested, we introduced nucleotide changes encoding: (*a*) the phenylalanine mutation L419:F; (*b*) the phenylalanine mutation R416:F; and (*c*) the charge mutations L419:R and R416:E, to examine the consequences of single residue changes in size, hydrophobicity and charge, respectively.

To investigate the behavior of these mutants in a cellular environment, we subcloned them into mammalian expression vectors and expressed them transiently in epithelial cell lines PtK2 and SCC-13. Some mutants (R416:E, R416:F, and L419:F) were indistinguishable from wild-type K14P, integrating without disruption into the endogenous keratin filament network (Fig. 8, *A* and *B*, transfected SCC-13 cells, anti-P, and anti-K5, respectively; *C* and *D*, transfected PtK2 cells, anti-P, and anti-K14, respectively). In contrast, L419:R caused withdrawal of the keratin network from the cell periphery and/or complete perinuclear collapse in >20% of transfected SCC-13 cells (*E* and *F*) and >50% of transfected PtK2 cells (*G* and *H*).

As expected, when these COOH-terminal rod mutants were tested in vitro, they all assembled with K5 into 10-nm filaments in vitro (Fig. 9). Once again, a correlation existed between the extent to which mutants perturbed keratin network formation in vivo with that observed in vitro. Thus,

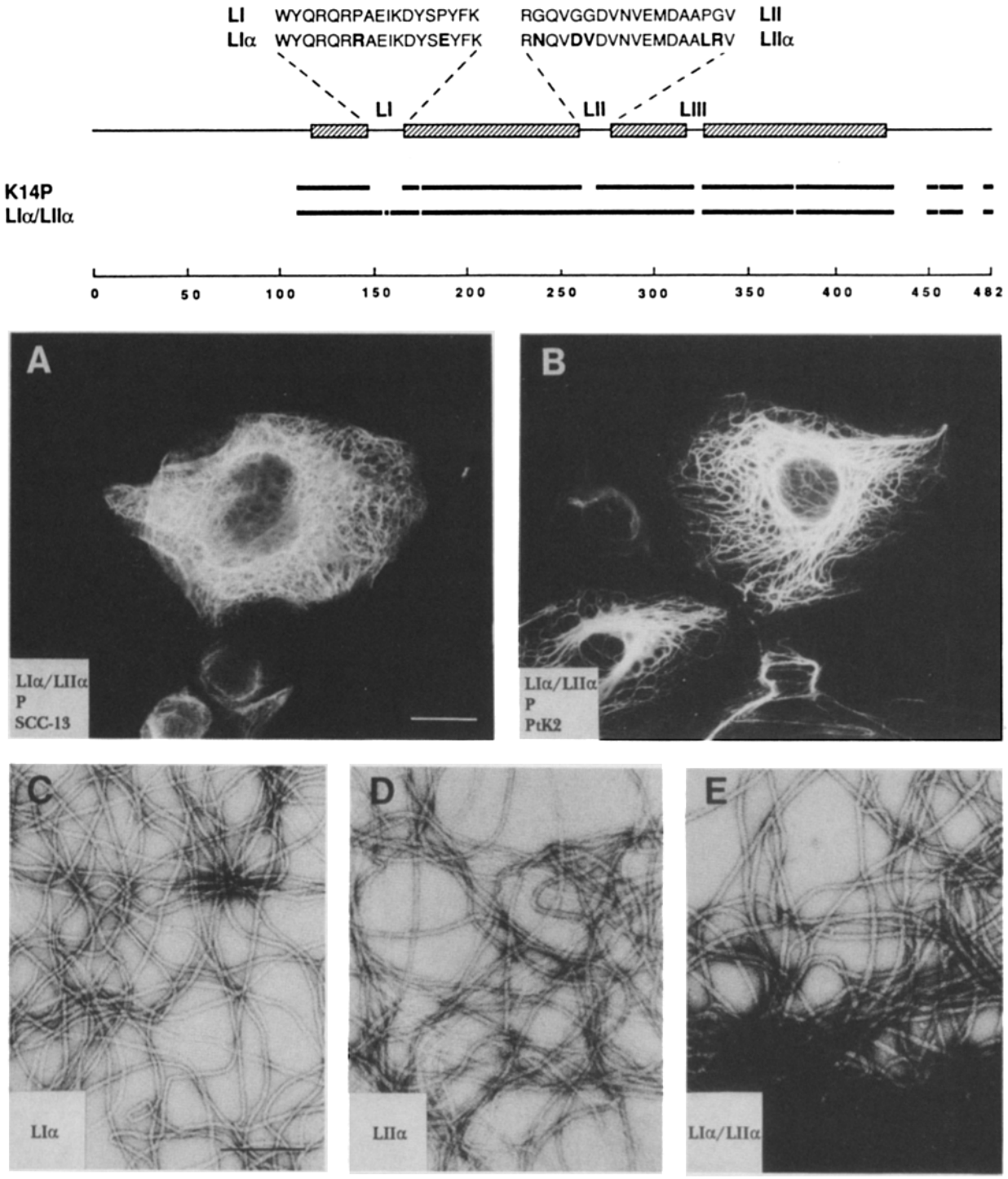

Figure 6. In vivo and in vitro consequences of removing the naturally occurring proline and glycine residues from the nonhelical linker regions of K14. A stick diagram at top denotes the amino acid substitutions made to create the linker mutants LIα, LIIα, and LIα/LIIα (the double linker mutant). Below, solid bars represent regions of the K14P and LIα/LIIα proteins predicted to be α-helical by the secondary structure prediction method of Garnier et al., 1978. Decision constants of −100 and 50 were assigned to the α-helical and extended chain conformation potentials, respectively, as suggested by Garnier et al., 1978. The numbers below the diagram correspond to amino acid residue numbers. *A* and *B* show SCC-13 (*A*) and PtK2 (*B*) cells transfected with LIα/LIIα and stained with anti-P. These wild-type phenotypes were also observed with the LIα and LIIα mutants. *C*, *D*, and *E* show filaments assembled by in vitro combination of K5 and either LIα, LIIα and LIα/LIIα, respectively. Note that in all three cases, the filaments were smooth and regular, but had a tendency to aggregate. This tendency was mild in the LIα (*C*) and LIIα (*D*) assembly assays, but was dramatic in the LIα/LIIα filaments (*E*). Filaments shown in *E* were on the edge of a large (>10 μm) electron-opaque ball of filaments. Nearly all of the K5-LIα/LIIα filaments formed from a 250 μg/ml mixture were clumped in a large aggregate visible to the eye. Bars: (*A* and *B*) 20 μm; (*C–E*) 200 nm.

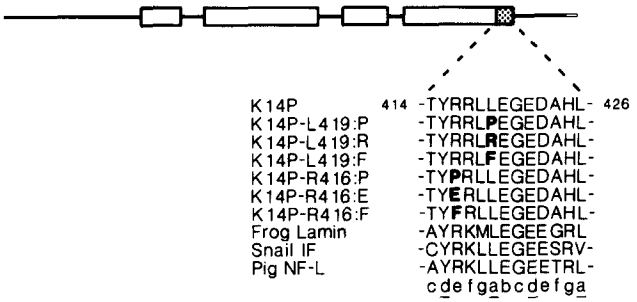

Figure 7. Stick diagram of point mutations at the carboxy end of helix 2B, depicting their location relative to the α-helical rod domain. The rod domain (see legend to Fig. 1) is denoted by boxes. The speckled region denotes the highly conserved carboxy end of helix 2B, whose sequences are provided. Thin black bars denote non-helical domains; thin white bar denotes the neuropeptide substance P tag. The mutant residues are indicated in bold. The high degree of sequence conservation between the end of helix 2B of K14 and other IF proteins can be appreciated by comparison with the corresponding segments of the most distantly related IF sequences: frog (Xenopus) lamin (Doring and Stick, 1990); snail (Helix asp.) cytoskeletal IF (Dodemont et al., 1990) and porcine low molecular weight neurofilament protein (Geisler et al., 1983). Beneath the sequences is an indication of the heptad repeats, where many a and d residues throughout the rod domain are hydrophobic. Point mutants were engineered by site-directed mutagenesis using either the Kunkel method (Kunkel, 1985), synthetic oligonucleotide inserts or polymerase chain reaction methods. In all cases, mutations were verified by DNA sequencing.

R416:E and L419:F produced filaments which were very similar to wild-type filaments (*A*). In contrast, L419:R generated relatively short filaments with more atypical features, including branching, diameter nonuniformity, and aggregation (*B* and *B'*; variation in filament diameter denoted by arrowheads in *B'*). Collectively, our results demonstrated that all point mutations in the very highly conserved end regions of the α-helical rod domain of K14 caused detectable perturbations on keratin IF assembly and filament forming efficiency. The most severe phenotypes were those generated by mutations involving loss of hydrophobicity or peptide backbone deformation.

Discussion

The Mean

All IF proteins have proline and glycine residues within three small and localized segments of the α-helical rod domain. While these residues almost certainly cause local perturbations in the helical rod, the rod nevertheless tolerates these structural aberrations and still permits coiled-coil formation (Hanukoglu and Fuchs, 1982, 1983; Geisler and Weber, 1982; Steinert et al., 1983). In fact, it has generally been predicted that given their defined locations, these helix-perturbing residues are somehow important and perhaps even essential for proper higher ordered interactions and filament assembly. Moreover, because of their evolutionarily conserved exclusion from the four α-helical domains of the rod, proline residues in the helical domains have been assumed to be deleterious to the formation of the coiled-coil and the assembly of subunits into 10-nm filaments. This notion has prevailed to such an extent that it had never been tested experimentally.

Indeed it was surprising to discover that proline mutants positioned throughout the central segments of the rod domain had significantly less severe effects on keratin structure and network formation than proline or more subtle mutations at the ends of the rod. Moreover, removal of the naturally occurring proline and glycine residues in the nonhelical linker domains had relatively minor effects on keratin filament network formation in vivo and on keratin filament assembly in vitro. Although none of the central residues chosen for mutagenesis was as highly conserved as those at the ends, all but one (N183) had conservative or no changes in >80% of published IF sequences. In addition, three of these residues were within the more highly conserved a or d positions of the heptad repeats of hydrophobic residues.

A natural question arising from our results is why internal proline mutations might influence keratin network formation to a lesser extent than mutations at the rod ends. One likely explanation is that proline-induced kinks or bends in the peptide backbone can be tolerated when embedded in a long stretch of stabilizing coiled-coil. While additional experiments will be necessary to test this notion, our data suggest that the large central coiled-coils of IF subunits are more flexible than previously realized, since they can absorb significant local alterations in the α-helix without compromising function. Are the short nonhelical linker regions simply a reflection of sequence segments best able to tolerate flexibility without loss of function? While this is possible, an alternative and intriguing possibility arising from our studies is that conservation of these linkers might be important for cytoskeletal architecture, rather than filament assembly per se. If the aggregation of linker mutant-generated filaments observed in vitro is relevant in vivo, then this could account for why these nonhelical segments occur in virtually all IF proteins. The absence of gross keratin network perturbations in cells expressing our linker mutants could not be a result of too low a keratin concentration within the epidermal cells, since keratins are present in these cells at ~5 mg/ml (unpublished), i.e., a greater concentration than that at which filament aggregation occurred in vitro. However, it could be that the endogenous keratins in transfected cells attenuated aggregation by the mutant. Finally, it could be that filament aggregation is more deleterious to a cell in the context of a tissue than in culture. Thus, while we observed little or no effects on filament assembly with mutants involving the introduction or removal of proline residues within the internal portions of the rod, subtle differences in either filament structure (internal proline mutants) or filament aggregation (linker mutants) might still give rise to subtle physiological aberrancies.

The Ends

Mutant-induced collapse of the keratin filament network was first observed in cells transfected with carboxy- and amino-terminal deletion mutants (Albers and Fuchs, 1987; 1989; Coulombe et al., 1990; Lu and Lane, 1990). However, since (*a*) deletions involved a nonhelical end as well as a carboxy- or amino-terminal segment of the rod, and (*b*) mutagenesis of other portions of the rod domain were not conducted, the special importance of these highly conserved end domains could not be appreciated from those studies. Indeed, the ba-

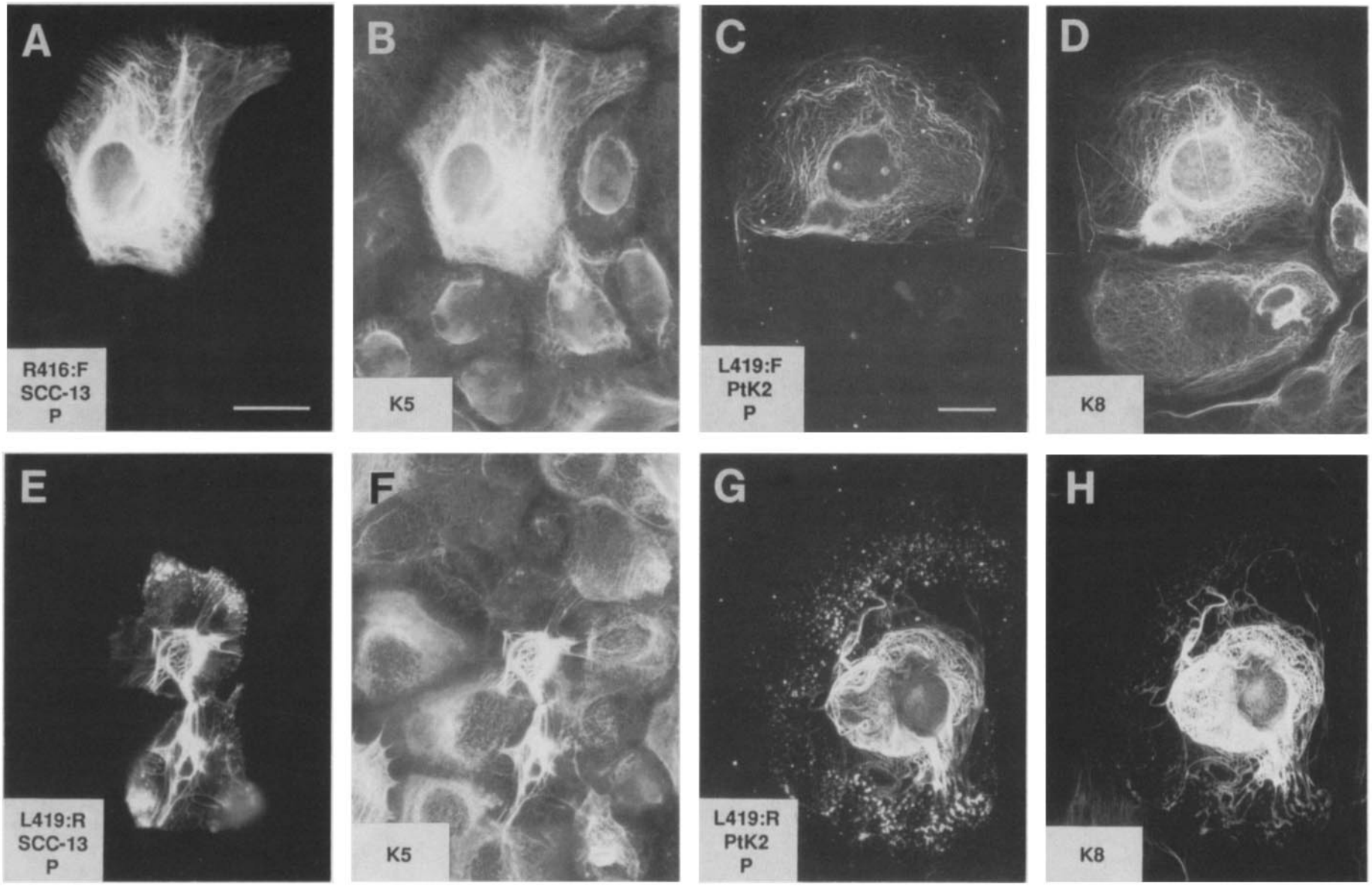
A
R416:F
SCC-13
P
B
K5
C
L419:F
PtK2
P
D
K8
E
L419:R
SCC-13
P
F
K5
G
L419:R
PtK2
P
H
K8

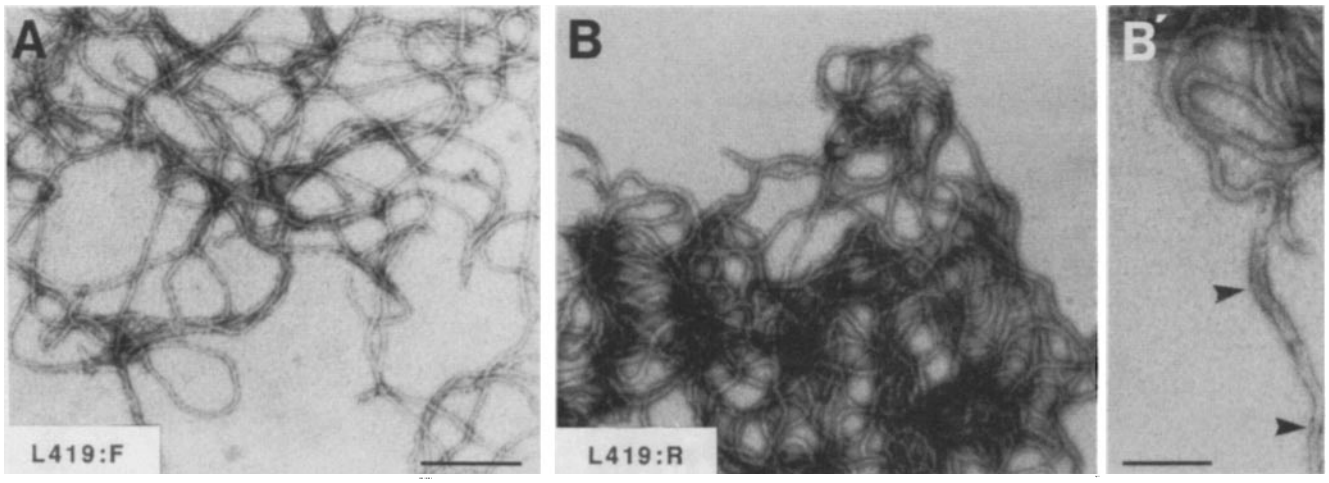

Figure 9. In vitro assembly of helix 2B mutants into 10-nm filaments. One mutant, R416:F, was susceptible to bacterial proteolysis and therefore was not used for in vitro studies. In vitro assembly and filament forming efficiency studies were carried out as described in the legend to Fig. 4. Filaments shown were assembled from K5 and the following: (*A*) (*B*) L419:F (note that filaments are near wild-type). This phenotype was also seen for R416:E. (*B*) L419:R (note marked aggregation of filaments, as well as non-uniform diameter and shortness). (*B'*) L419:R, higher magnification to visualize irregularity in filament width, denoted by arrowheads. Bars: (*A*) 200 nm; (*B'*) 100 nm.

sis for the collapsed network phenotype seems to reside predominantly in ends of the rod rather than in the internal portions of the rod or in the nonhelical segments flanking the rod. Moreover, since those mutants that caused the most dramatic changes in filament structure in vitro were the same that caused IF network collapse in vivo, it seems likely that the in vivo aberrations were caused by structural abnormalities originating in these ends. That the network withdraws from the cell periphery implies that the keratin network is more sensitive here than elsewhere to the structural perturbations introduced by the mutations. We do not yet know whether this reflects an inherent difference in stability between the keratin network at the periphery versus elsewhere, or alternatively, whether a membrane–IF interaction exists which is especially sensitive to changes in IF structure.

It is striking that a collapse of the keratin filament network was generated by all of the five different proline substitutions in helix 1A and at the end of helix 2B. Surprisingly, however, some mutations at the COOH-terminal end of the rod (R416:E, L419:F, and R416:F) were without major effect in vivo or in vitro, despite the fact that these residues were highly conserved and that two of these mutations changed the hydrophobicity and/or the charge of the residue. That such substantial side chain variation can be tolerated is further documented by the recent finding of an arginine to glutamic acid substitution at the 416 equivalent position of a Drosophila lamin (Osmon et al., 1990). Collectively, these data indicate that whether natural or artificial, substantial changes in the side chains of these critical end sequences can sometimes be tolerated. In contrast, proline mutations, which alter the peptide backbone as well as the side chain, cannot. The constraint of conformation imposed by a proline mutation will locally disrupt or at least kink the α-helical structure at the rod end (Chou and Fasman, 1978). In the absence of a stabilizing α-helix flanking both sides of this aberration, such a change might perturb IF structure to even a greater extent than deletion of these residues. This notion is consistent with our findings that proline mutations at the COOH-terminal end of the rod were more deleterious than deletion (Coulombe et al., 1990). Thus our findings imply that the specific contacts normally associated with residues at the ends of the rod are not as important for function as the underlying α-helical structure. These findings exclude the possibility that the sole purpose for the highly conserved end domains is for specific interactions between intermediate filament-associated proteins (IFAP) rather than for keratin filament assembly per se.

It is possible that the conditions we have used to assay the effects of our mutants on keratin network formation and IF assembly were less severe than those that exist in nature. For instance, it has recently been observed that the flattened shape of cultured epidermal cells seems to stabilize the cytoplasmic keratin network in a fashion that does not occur in the physiological context of the skin (Coulombe et al., 1991*a*). Moreover, the in vitro assembly conditions may be more permissive to subtle structural perturbations than filament assembly in vivo. Thus, although all of our mutants exhibited at least subtle defects in their ability to influence ker-

Figure 8. Immunofluorescence analysis of cells transfected with helix 2B mutant keratins. SCC-13 and PtK2 cells were transfected with keratin point mutants in the highly conserved carboxy terminal end of helix 2B. Cells were fixed and stained as in the legends to Figs. 2 and 3. The first of each set was stained with anti-P and the second with either anti-K5 (*SCC-13*) or anti-K8 (*PtK2*). SCC-13 cell expressing R416:F (*A* and *B*) or PtK2 cell expressing L419:F (*C* and *D*). Note: mutants L419:F and R416:E were indistinguishable from R416:F which was indistinguishable from wild-type K14P, and exhibited the shown phenotype in >90% of transfected PtK2 cells, and >99% of transfected SCC-13 cells. SCC-13 cell (*D–F*) or PtK2 cell (*G* and *H*) expressing L419:R. Note that the keratin network is collapsed around the nucleus, with punctate staining at the periphery. Bars, 20 μm.

atin filament assembly, the range of their effects in vivo may be more severe. Recent K14 mutational studies from a genetic skin disease involving K14 mutations suggest that this may be the case (see below).

Relevance to Other IFs

In the past few years, a number of deletion and two point mutagenesis studies have been conducted on a variety of different IF proteins (Albers and Fuchs, 1987, 1989; Christian et al., 1990; Coulombe et al., 1990; Gill et al., 1990; Hatzfeld and Weber, 1990*a*,*b*; Heald and McKeon, 1990; Lu and Lane, 1990; Wong and Cleveland, 1990). Thus far, IF mutageneses have been largely confined to nonhelical head and tail domains or to the end domains of the rod, and hence there are very little data which might enable us to assess the extent to which our results on the internal segments of the K14 rod will be relevant to other IF proteins. However, two lines of evidence suggest that the effects of analogous rod mutations in other non-keratin IF proteins may be more severe: one is that keratins are obligatory heteropolymers (Franke et al., 1983); the other is that keratin heterodimers and heterotetramers are significantly more stable than other IF subunits (Coulombe and Fuchs, 1990). This said, the extraordinary conservation of 10-nm assembly, structure and sequence among IF proteins makes it very likely that the range of severities observed with our point mutants will also hold for other IF proteins, even though the scale of severity may vary. Consistent with this notion are the studies of Heald and McKeon (1990), who tested the ability of point mutations in lamin A to influence nuclear lamina formation in transfected cells in culture. While these researchers only scored the ability to form or disrupt the lamina, and did not conduct in vitro assembly studies, they did demonstrate that the lamin equivalent of R416:P caused disruption of the nuclear lamina, in a fashion perhaps analogous to that which we observed for the keratin network. In addition, albeit more conservative than our internal proline mutations, two internal point mutations in helix 2B were without effect on lamina network formation. It is notable that an hypothesis derived from the lamin studies suggested that residues a, d, e, and f in the heptad repeat may be the most sensitive sites for amino acid substitutions, since these residues point inward in the coiled-coil interaction (Heald and McKeon, 1990). While our data do not discount this notion, it is notable that all four of our internal proline mutations were in a or d positions, and yet these did not alter dimer or tetramer formation, nor did they appreciably perturb filament assembly. As further studies on lamins, keratins, and other IF proteins are conducted, the extent to which their coiled-coil domains can accommodate similar substitutions should become more apparent.

When all of the data are taken together, a picture emerges whereby 10-nm filament structure can tolerate considerable flexibility in amino acid sequence, particularly within the very stable central coiled-coil segments of the rod domain. The substitution of different residues affects IF formation and stability to varying degrees, and while some mutations may be tolerated within the framework of the 10-nm filament, others, particularly α-helical perturbing mutations in the ends of the rod, cannot. The fact that maintenance of a specific structure at the rod ends is so vital to IF assembly and function explains why these sequences have been so highly conserved throughout evolution.

Relevance to Epidermolysis Bullosa Simplex

The finding that certain mutations have more severe effects than others on IF stability, structure, and network formation has important implications for a class of autosomal dominant, human blistering skin diseases known as EBS. EBS has recently been shown to arise from genetic mutations in basal epidermal keratin genes (Vassar et al., 1991; Coulombe et al., 1991*a*,*b*; Bonifas et al., 1991). In patients with EBS, keratin filament elongation is restricted, and this apparently leads to epidermal cell fragility and cytolysis upon mild incidental trauma (Coulombe et al., 1991*b*). Interestingly, in two human cases of the most severe (Dowling Meara) form of the disease, a single amino acid, R125, near the amino terminal end of the K14 rod domain was mutated to either a cysteine (R125:C) or a histidine (R125:H) (Coulombe et al., 1991*b*). In contrast, a patient with a milder form (Koebner) of EBS was found to have the point mutation L384:P, located in an internal segment of the K14 rod (Bonifas et al., 1991). Bonifas et al. (1991) assumed that a proline mutation within the rod would disrupt the α-helix in a fashion analogous to previous deletion mutations at the rod ends. In contrast, if the L384:P mutation is responsible for the EBS phenotype, as it has been shown for the R125:C mutation (see Coulombe et al., 1991*b*), then our present data predicts that the L384:P would be significantly more subtle in its phenotype than either (*a*) rod-end deletions or (*b*) a number of different rod-end point mutations. Therefore, our data provide an insight into why the EBS blistering disease might be milder in a patient harboring an L384:P mutant than in one with either R125:C or R125:H mutations. Although we have not yet assayed L384:P in our system, this mutation is in the "a" residue of the heptad immediately adjacent to the heptad containing the V380:P "d" residue mutation that we have described in this paper. Thus, L384:P might be expected to behave similarly to V380:P. More generally, we anticipate that most K14 mutations in Dowling Meara patients will be located in the more critical end domains, whereas most K14 mutations in patients with milder forms of EBS will be located in more internal segments of the rod. As additional EBS patients and K14/K5 point mutations are characterized, the extent to which this holds true should become apparent. Finally, the striking similarities in structure among all IF types, coupled with the knowledge that perturbations in keratin networks can lead to human disease opens the intriguing possibility that other as yet unidentified diseases in other tissues may have as their basis perturbations in other IF networks caused by mutations in IF sequence.

A special thank you goes to Philip Galiga for his artful presentation of the data, and to Dr. Kathryn Albers, Dr. Raphael Kopan, Dr. Gerhard Wiche, Dr. Tom Terwilliger, and Mary Beth McCormick for their generous and helpful advice and for assistance in various technical phases of the work. Finally, we thank Dr. Barry Eckert (State University of New York, Buffalo, NY) for his helpful suggestions concerning IF assembly conditions. This work was supported by a grant from the National Institutes of Health. P. A. Coulombe is the recipient of a Centennial fellowship from the Medical Research Council of Canada. A. Letai is a pre-doctoral trainee supported by the National Cancer Institute and the Medical Scientist's

Training Program. E. Fuchs is an investigator of the Howard Hughes Medical Institute.

Received for publication 23 August 1991 and in revised form 25 November 1991.

References

Aebi, U., M. Haner, J. Troncoso, R. Eichner, and A. Engel. 1988. Unifying principles in intermediate filament (IF) structure and assembly. *Protoplasma.* 145:73–81.

Albers, K., and E. Fuchs. 1987. The expression of mutant epidermal keratin cDNAs transfected in simple epithelial and squamous cell carcinoma lines. *J. Cell Biol.* 105:791–806.

Albers, K., and E. Fuchs. 1989. Expression of mutant keratin cDNAs in epithelial cells reveals possible mechanisms for initiation and assembly of intermediate filaments. *J. Cell Biol.* 108:1477–1493.

Bonifas, J. M., A. L. Rothman, and E. H. Epstein. 1991. Epidermolysis Bullosa Simplex: Evidence in two families for keratin gene abnormalities. *Science (Wash. DC).* 254:1202–1205.

Choi, Y., and E. Fuchs. 1990. TGF-beta and retinoic acid: regulators of growth and modifiers of differentiation in human epidermal cells. *Cell Regul.* 1:791–809.

Chou, P. Y., and G. D. Fasman. 1978. Prediction of the secondary structure of proteins from their amino acid sequence. *Adv. Enzymol.* 47:45–148.

Christian, J. L., N. G. Edelstein, and R. T. Moon. 1990. Overexpression of wild-type and dominant negative mutant vimentin subunits in developing xenopus embryos. *New Biol.* 2:700–711.

Conway, J. F., and D. A. D. Parry. 1988. Intermediate filament structure: 3. Analysis of sequence homologies. *Int. J. Biol. Macromol.* 10:79–98.

Coulombe, P., and E. Fuchs. 1990. Elucidating the early stages of keratin filament assembly. *J. Cell Biol.* 111:153–169.

Coulombe, P., Y.-M. Chan, K. Albers, and E. Fuchs. 1990. Deletions in epidermal keratins that lead to alterations in filament organization and assembly: in vivo and in vitro studies. *J. Cell Biol.* 111:3049–3064.

Coulombe, P. A., M. E. Hutton, R. Vassar, and E. Fuchs. 1991*a*. A function for keratins and a common thread among different types of Epidermolysis Bullosa Simplex Diseases. *J. Cell Biol.* 115:1661–1674.

Coulombe, P. A., M. E. Hutton, A. Letai, A. Hebert, A. Paller, and E. Fuchs. 1991*b*. Point mutations in human keratin 14 genes of Epidermolysis Bullosa Simplex patients: genetic and functional analyses. *Cell.* 66:1301–1311.

Dodemont, H., D. Riemer, and K. Weber. 1990. Structure of an invertebrate gene encoding cytoplasmic intermediate filament (IF) proteins: implications for the origins and the diversification of IF proteins. *EMBO (Eur. Mol. Biol. Organ.) J.* 9:4083–4094.

Doring, V., and R. Stick. 1990. Gene structure of nuclear lamin LIII of Xenopus laevis: a model for the evolution of IF proteins from a lamin-like ancestor. *EMBO (Eur. Mol. Biol. Organ.) J.* 9:4073–4081.

Franke, W. W., D. L. Schiller, M. Hatzfeld, and S. Winter. 1983. Protein complexes of intermediate-sized filaments: melting of cytokeratin complexes in urea reveals different polypeptide separation characteristics. *Proc. Natl. Acad. Sci. USA.* 80:7113–7117.

Garnier, J., D. J. Osguthorpe, and B. Robson. 1978. Analysis of the accuracy of and implications of simple methods for predicting the secondary structure of globular proteins. *J. Mol. Biol.* 120:97–120.

Geisler, N., and K. Weber. 1982. The amino acid sequence of chicken muscle desmin provides a common structural model for intermediate filament proteins. *EMBO (Eur. Mol. Biol. Organ.) J.* 1:1649–1656.

Geisler, N., E. Kaufmann, S. Fischer, U. Plessmann, and K. Weber. 1983. Neurofilament architecture combines structural principles of intermediate filaments with carboxy-terminal extensions increasing in size between triplet proteins. *EMBO (Eur. Mol. Biol. Organ.) J.* 2:1295–1302.

Gill, S. R., P. C. Wong, M. J. Monteiro, and D. W. Cleveland. 1990. Assembly properties of dominant and recessive mutations in the small mouse neurofilament (NF-L) subunit. *J. Cell Biol.* 111:2005–2019.

Graham, F. L., and Eb, E. van der. (1973). A new technique for the assay of infectivity of human adenovirus 5 DNA. *Virology.* 52:456–467.

Hanukoglu, I., and E. Fuchs. 1982. The cDNA sequence of a human epidermal keratin: divergence of sequence but conservation of structure among intermediate filament proteins. *Cell.* 31:243–252.

Hanukoglu, I., and E. Fuchs. 1983. The cDNA sequence of a type II cytoskeletal keratin reveals constant and variable structural domains among keratins. *Cell.* 33:915–924.

Hatzfeld, M., and W. W. Franke. 1985. Pair formation and promiscuity of cytokeratins: formation in vitro of heterotypic complexes and intermediate-sized filaments by homologous and heterologous recombinations of purified polypeptides. *J. Cell Biol.* 101:1826–1841.

Hatzfeld, M., and K. Weber. 1990*a*. The coiled coil of in vitro assembled keratin filaments is a heterodimer of type I and II keratins: use of site-specific mutagenesis and recombinant protein expression. *J. Cell Biol.* 110:1199–1210.

Hatzfeld, M., and K. Weber. 1990*b*. Tailless keratins assemble into regular intermediate filaments in vitro. *J. Cell Sci.* 97:317–324.

Hatzfeld, M., and K. Weber. 1991. Modulation of keratin intermediate filament assembly by single amino acid exchanges in the consensus sequence at the C-terminal end of the rod domain. *J. Cell Sci.* 99:351–362.

Hatzfeld, M., G. Meier, and W. W. Franke. 1987. Cytokeratin domains involved in heterotypic complex formation determined by in vitro binding assays. *J. Mol. Biol.* 97:237–255.

Heald, R., and F. McKeon. 1990. Mutations of phosphorylation sites in lamin A that prevent nuclear lamina disassembly in mitosis. *Cell.* 61:579–589.

Kunkel, T. A. 1985. Rapid and efficient site-specific mutagenesis without phenotypic selection. *Proc. Natl. Acad. Sci. USA.* 82:488–492.

Lane, E. B. 1982. Monoclonal antibodies provide specific intramolecular markers for the study of epithelial tonofilament organization. *J. Cell Biol.* 92:665–673.

Lu, X., and E. B. Lane. 1990. Retrovirus-mediated transgenic keratin expression in cultured fibroblasts: specific domain functions in keratin stabilization and filament formation. *Cell.* 62:681–696.

Marchuk, D., S. McCrohon, and E. Fuchs. 1984. Remarkable conservation of structure among intermediate filament genes. *Cell.* 39:491–498.

Nelson, W., and T.-T. Sun. 1983. The 50- and 58-kdalton keratin classes as molecular markers for stratified squamous epithelia: cell culture studies. *J. Cell Biol.* 97:244–251.

Osman, M., M. Paz, Y. Landesman, A. Fainsod, and Y. Gruenbaum. 1990. Molecular analysis of the Drosophila nuclear lamin gene. *Genomics.* 8: 217–224.

Pruss, R. M., R. Mirsky, M. C. Raff, R. Thorpe, A. J. Dowding, and B. H. Anderton. 1981. All classes of intermediate filaments share a common antigenic determinant defined by a monoclonal antibody. *Cell.* 27:419–428.

Steinert, P. M. 1990. The two-chain coiled-coil molecular of native epidermal keratin intermediate filaments is a type I-type II heterodimer. *J. Biol. Chem.* 265:8766–8774.

Steinert, P. M., and D. R. Roop. 1988. Molecular and cellular biology of intermediate filaments. *Annu. Rev. Biochem.* 57:593–625.

Steinert, P. M., R. H. Rice, D. R. Roop, and B. L. Trus, A. C. S. 1983. Complete amino acid sequence of a mouse epidermal keratin subunit and implications for the structure of intermediate filaments. *Nature (Lond.).* 302:794–800.

Vassar, R., P. A. Coulombe, L. Degenstein, K. Albers, and E. Fuchs. 1991. Mutant keratin expression in transgenic mice causes marked abnormalities resembling a human genetic skin disease. *Cell.* 64:365–380.

Weber, K., U. Plessmann, and W. Ulrich. 1989. Cytoplasmic intermediate filament proteins of invertebrates are closer to nuclear lamins than are vertebrate intermediate filament proteins: sequence characterization of two muscle proteins of a nematode. *EMBO (Eur. Mol. Biol. Organ.) J.* 8:3221–3227.

Wong, P. C., and D. W. Cleveland. 1990. Characterization of dominant and recessive assembly-defective mutations in mouse neurofilament NF-M. *J. Cell Biol.* 111:1987–2003.

Wu, Y.-J., and J. G. Rheinwald. 1981. A new small (40 kd) keratin filament protein made by some cultured human squamous cell carcinoma. *Cell.* 25:627–635.